COBEM 2021 26th International Congress of Mechanical Engineering
November 22-26, 2021, Virtual Congress, Brazil

COB-2021-1274
FINITE ELEMENT METHOD APPLIED TO MODEL THE STRUCTURAL STIFFNESS BEHAVIOUR OF A MACHINE TOOL

Tédni de Abreu Goulart
Jefferson de Oliveira Gomes
Ronnie Rodrigo Rego
Instituto Tecnológico de Aeronáutica – ITA / Centro de Competência em Manufatura – CCM
tedni@ita.br
gomes@ita.br
ronnie@ita.br

Abstract. *The current trends of the industry have demanded parts with more complex shapes, which also demand more accurate machine tools. Many error sources can influence the machine's accuracy; Among those, the static and dynamic loads act on the machine's structure, causing deflections that directly affect its behavior. The objective of this study is to understand how the accuracy of a machine tool is influenced by its structural stiffness behavior. The structural stiffness of each translational machine axis was mapped in the entire machine's work volume. This investigation used a finite element model to map the directional stiffness of the axes. All the investigation procedure was executed in a five-axis machining center. With the results of the finite element model, a structural stiffness map was established for any point of the machine's work volume. The correlation between machine tool structure and the stiffness map can be established and different machining strategies can be derived based on this correlation. The developed procedure proved to be a robust method to understand the structural behavior of a machine tool and which, due to the process loads, must be considered to increase the final process accuracy.*

Keywords: *Machine tools, Structural stiffness, Accuracy, Machining process.*

1. INTRODUCTION

Machine tools represent the capacity of a nation to produce consumer goods. In the current industry, most manufacturing processes are performed by a machine tool, thus its relevance for human life is undeniable. Nowadays, the concepts of Industry 4.0 require machine tools with higher performance levels, which according to Weck (1984) and Brecher and Witt (2004), is mainly influenced by its positional accuracy. Therefore, understanding how it behaves is essential to achieve performance improvement.

1.1 Positional accuracy evaluation

Considering the number of mechanical elements related to the axes' movement of a machine tool, many error sources can influence its positional accuracy. These error sources act at the machine's structure causing deformations in the structural loop, which are defined by the standard ISO 230-1 (2012) as: "assembly of components which maintains the relative position and orientation between two specified objectives". For this reason, the analysis of the structural loop is defined in the literature as indicative of the positional accuracy of a machine tool (Huo, Cheng, and Wardle 2009; Abele et al. 2013; Szipka, Laspas, and Archenti 2018).

The analysis of the structural loop is related to the evaluation of its deflection rate under defined axes position and input loads (i.e. mechanical and thermal loads). The capacity of the structural loop to resist the deflections caused by the applied loads is defined as structural stiffness. Thus, the lower the deflection rate of the structural loop, the higher is the structural stiffness of the machine tool at this specific situation. The deformation in the structural loop caused by an input load is measured directly at the Tool Center Point (TCP) of the machine tool. In this case, the structural stiffness of a machine tool can be defined by measuring the deflection of the TCP under the application of a defined input load. Figure 1 shows a draft of the structural loop for the machine tool analyzed at the present study and an example of deflection in X and Y directions.

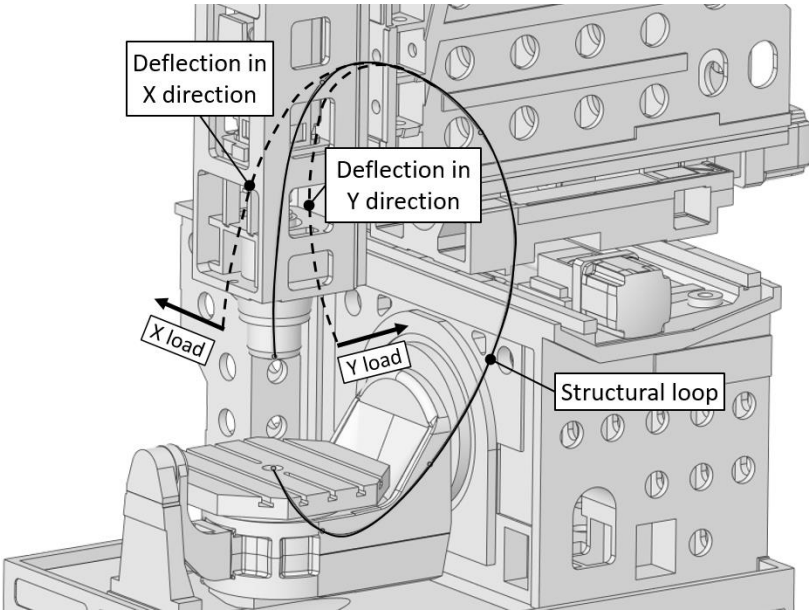

Figure 1. Example of structural loop deflection in X and Y direction.

Once the machining process is executed under different input loads with different value ranges, this deflection is related to the positional accuracy of the machine tool. For this reason, structural stiffness is defined in the literature as the most important parameter in a machine tool. Koenigsberger (1970) declares "[…]if the stiffness affects the accuracy of alignment and guidance of the various parts under the working loads, it becomes the most important parameter".

1.2 Virtual and computational models

Decisions about the machine's stiffness are taken during the design phase, and the resultant machine's performance is a consequence of these decisions. During this phase, virtual models are applied to define the characteristics of the machine tool structure and architecture. However, the virtual machine tool concept has been combined with experimental procedures to better understand the machine behavior and be able to optimize its positional accuracy (Archenti 2014).

Archenti (2014) used a computational model of a machine tool combined with experimental tests to predict the path deviations and correlated with machining operation in a specific region of the machine's work volume. In this study, experimental tests were correlated with a planar map of the machine's stiffness, not considering the movements of the machine's vertical axis is established. Szipka, Laspas, and Archenti (2018) combined two modeling methods to predict the machine's error under loaded conditions. Gao *et al.* (2016) and Deng *et al.* (2017) proposed a similar approach, but in these cases, the entire volume was considered, and therefore, it was possible to define the machine's stiffness for any point of the work volume.

Bearing this in mind, the present paper has the objective of defining a method for a model construction that would be able to identify how significantly the axes movements affect the structural stiffness of the machine tool. By developing this model, experimental tests can be better proposed based on simulations using the model to validate. Also based on stiffness behavior, resultant from the virtual model, different machining procedures can be proposed to increase the machine's positional accuracy.

2. CONSTRUCTION OF MACHINE TOOL FEM MODEL

The modeling process, which was performed to complete the machine's FEM (Finite Element Method) model, is summarized in Figure 2a as a workflow. After the construction of the model, structural simulations were performed to investigate the stiffness behavior of the machine tool in its entire work volume. All the investigation procedure was executed in a ROMI DCM 620 5X five-axis machining center.

Due to the high number of components and contact among them, the machine tool was divided into sub-models to simplify the model's development and geometric discretization. To have a final model of the entire machine, each sub-model is developed separately and then coupled to the other sub-model considering the proper interactions. This division decreases complexity and enables a gradual construction and test of the complete model.

The complete model was divided into five sub-models. Figure 2b shows the machine tool division and each submodel structure. The models were elaborated following three main steps, geometry discretization, imposition of boundary conditions, and evaluation of the results.

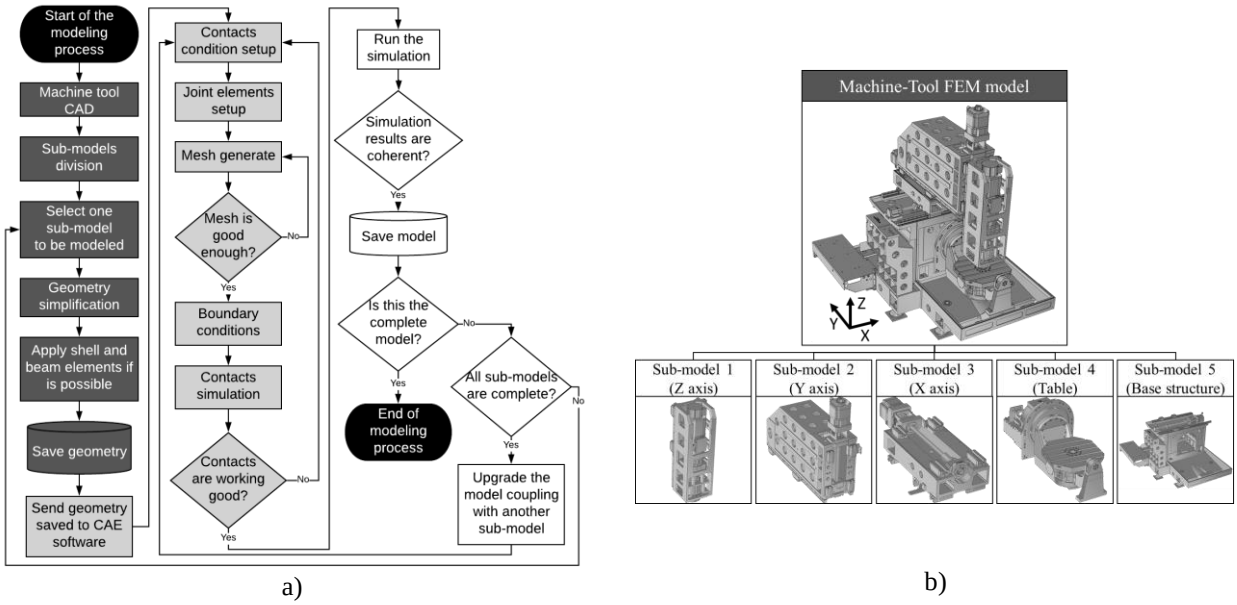

Figure 2. a) Workflow for machine tool complete FEM modeling process; b) Structure of the complete and sub-models of the machine tool.

Geometry discretization started with the preparation of the machine tool's computer-aided design (CAD) model. The division of the sub-models (Figure 2b) was elaborated to allocate each primary moveable part in a different sub-model. The connections among the sub-models were performed by a joint element on the CAE software. Geometry simplification was executed by excluding chamfers smaller than 5 mm, rounds smaller than 10 mm, all fasteners, holes smaller than 20 mm, and non-structural pieces e.g. sheet metal covers. This can be applied because these elements do not have a significant influence on the final stiffness of the model.

The definition of the most suited contact condition is based on the actual physical interaction between parts. In this case, considering that in a real situation the components of each sub-models are rigidly fixed to each other; therefore, a bonded contact condition was applied. The material properties were then defined according to the correspondent machine tool part. Since the drives, spindle, and table are not completely known, they were defined as equivalent density material. With this approach, the equivalent weight and inertial moment are considered at the FEM model. The material of each part as well as its mechanical properties are detailed in Table 1, the Young's modulus was defined based on the values presented by Zulaika and Campa (2009).

Table 1. Material properties (Zulaika and Campa 2009).

Machine's parts	Material	Density	Young's modulus
Axes drives	-	4000 kg/m^3	50 GPa
Spindle drive	-	2800 kg/m^3	50 GPa
Spindle	-	6500 kg/m^3	50 GPa
Table	-	6300 kg/m^3	50 GPa
Casted structure	GG 25	7200 kg/m^3	120 GPa
Non-casted parts (e.g. linear guides, ball screw)	Steel	7850 kg/m^3	210 GPa

After defining the contact between fixed parts and the material properties, all joint elements that connect movable parts in the same sub-model and between two different sub-models were defined. Aiming to simulate the connections in a real situation (e.g. linear guides, ball screws, and bearings) implementing customized joint properties, they were defined using a command line.

The meshing of each sub-model and the complete model was generated from an initial automatically generated mesh, which was then modified. In general, three global element sizes were used to mesh the model and the drivers were defined as rigid, consequently, they were not meshed. This was considered because the drivers have no structural function, but its inertia can influence in the structural behavior of the machine. The parts discretized using each element size were separated into groups, depicted in Figure 3a. The element size of each group was defined using the mesh quality tool available on the software, and to conclude it, a test of mesh convergence was performed. The mesh converged after two

iterations with a variation of 0.96% of the TCP total deformation. The final mesh for the complete model is presented in Figure 3b.

a) b)

Figure 3. a) Mesh groups and b) final mesh of the complete model.

By achieving the desired mesh quality, the loads and supports conditions were defined. To simulate the stiffness behavior in the entire machine's volume, in the complete model, fifteen different conditions changing the TCP position were tested. In all fifteen setups, the input force value was defined as 1 kN in each direction X, Y, and Z. This force value was defined to obtain the directional deformation results in terms of μm/N, which correspond to the axis compliance level simplifying the comparison of their stiffness.

The fifteen conditions tested are shown in Figure 4a. The points shown are positioned at the limit of the machine's work volume, which is represented by the transparent cylinder. For all these points, fixed support between the machine and ground was applied, restraining all degrees of freedom (DoF's) at the machine supports. This boundary condition was defined only for the complete model.

For the sub-models, a free-free modal analysis was performed just to check the contact conditions and joint elements of the sub-models. Since its results are the first six rigid body's modes shapes, the corresponding frequency values should be close to zero, which ensures that the sub-model connections/interactions are functional.

For the complete model, a free-free, modal analysis was also performed to identify any non-functional connection. A second verification was executed using a tool available in the software, the "contact tool", which shows all contact status in five categories: open, far open, gap, penetration and closed. After all, contacts been checked and eventually corrected, the model was solved.

For future reference, all performed tests using the FEM model were named according to its position on the machine's work volume, the name of each test point is summarized in Figure 4b. To compare the stiffness of each point, the central point (i.e. T10) was defined as the origin point, thus, its coordinates are X=Y=Z=0. The volume of the machine tool has a diameter of 520 mm and a high of 330 mm. Therefore, depending on the moving direction, the coordinate of any point from the central point will be varying ±165 mm in the Z direction and ±260 mm in the X and Y direction. For example, the coordinates of point T2 are X=0 mm, Y=260 mm, and Z=165 mm.

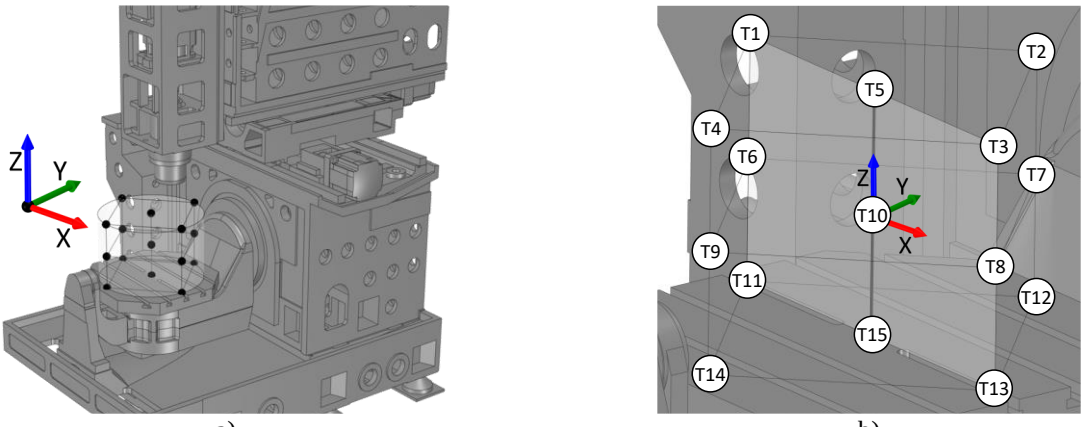

a) b)

Figure 4. a) TCP positions simulated with an input force of 1 kN value in each direction X, Y, and Z; b) Name and position of each test point in the machine's work volume.

3. RESULTS AND DISCUSSIONS

With the results for each simulated point, it was possible to compare the stiffness for each axis for the entire work volume. The FEM model was not validated using experimental techniques; thus, the stiffness value does not correspond to the machine's real stiffness. However, the stiffness variation between two different points can be considered to evaluate the influence of the axes' movement on the structural stiffness.

For the selected machine, the stiffness regarding loads applied in the Y direction is higher when comparing to loads applied in the X direction. It can be demonstrated by comparing the deflection resistance of the structural loop in each direction. According to Slocum (1992) and Soons (1993), the structural loop is a rapid way to evaluate the machine's stiffness and usually larger structural loops lead to lower resistance to deflection and consequently lower stiffness level.

In most machine tools, the structural loop is affected by the axes' movement, which also causes a stiffness change along with the movement. This is explained mainly because the point where the loads are applied changes and by modifying the distance along each axis, the corresponding torsion/bending moment is also modified. For the selected machine tool, this was confirmed from the results of the simulation tests.

The results will be presented in two different groups. The first presents the results for a constant position of the X axis, exactly at the center of the table (i.e. X=0). The second presents the results with the Y axis position kept at the center of the table (i.e. Y=0). Referring to Figure 4b the points which correspond to the first group are T2, T4, T5, T7, T9, T10, T12, T14, and T15. The respective names and positions in the machine's work volume for all these tests are presented in Figure 5a. The maximum and minimum stiffness for the X=0 condition, T2 and T14 respectively, are presented in Figure 5b.

For all these cases, where X was at position zero, the input loads in the Y direction do not cause any moment in the Z axis, only causing bending moment in the X axis. However, the input loads in the X direction cause a torsion moment in both Z and Y axes. The Z torsion moment increases as the Y axis moves towards the negative direction, and the Y torsion moment increases as the Z axis moves towards the negative direction. As both Z and Y torsion moments increase when the axes move from point T2 to point T14, the higher value for stiffness at point T2 was expected.

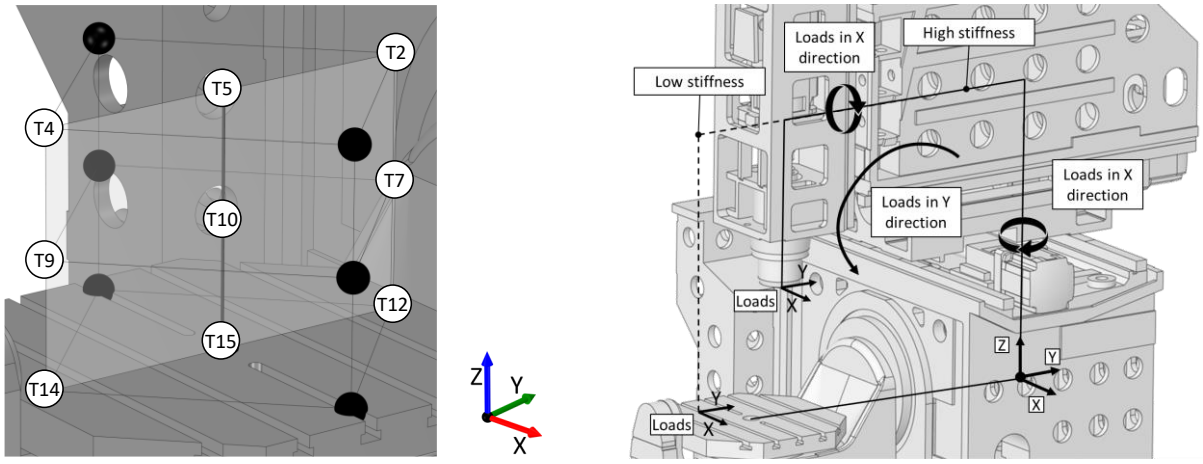

Figure 5. a) Name and position of the tests with X axis positioned in the center of the table; b) Points T2 and T14, an example of two different load conditions according to the Y and Z axes movement.

To better compare the stiffness variation of these points according to the movements of the Z and Y axes, the central point (i.e. T10) was taken as the reference stiffness value. The absolute value and the variation for all points are presented in a right view of the machine tool in Figure 6. The absolute value is presented in terms of N/μm and the variation is presented in terms of percentage increase or decrease when compared to the reference point.

Based on the results, is possible to see that the stiffness in the X axis direction is influenced by the movement in the Z direction in the entire work volume. However, for the test points T2, T7, and T12, the Z movement has more influence than in the other points. Still, regarding the stiffness in the X direction, it is also affected by the Y axis movement in the entire work volume. However, this influence is even higher for the points T2, T4, T5, T7, T9, and T10. These observations can also be seen in Figure 7 as well as in the results presented in Figure 6 for the X direction.

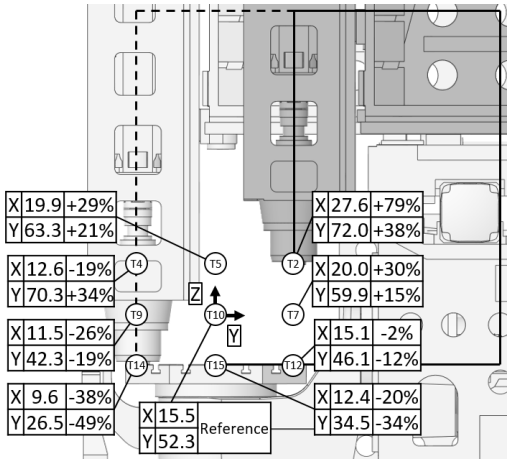

Figure 6. Stiffness absolute value in terms of N/µm and its variation in % for all points where the X axis is positioned in the center of the machine's work volume.

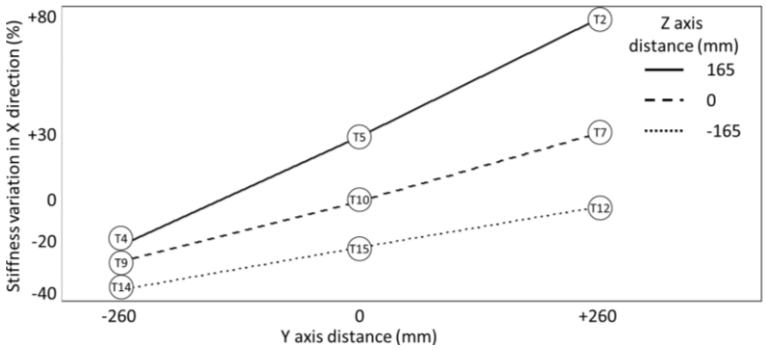

Figure 7. Influence of the interaction between the positioning of Y and Z axes in the stiffness in the X direction.

Considering the stiffness in the Y direction, the movement of both the Z and Y axes influences its final value. With the Y axis positioned in the points T4, T9, and T14 the stiffness level is highly influenced by the Z axis movement. This influence is also observed for the Y axis in intermediate (T5, T10, and T15) and highest position (T2, T7, and T12); however, the Z movement influence is reduced when the Y axis moves toward the negative direction (T4, T9, and T14).

The Y axis movement has a similar influence on the stiffness level when the Z axis is in the bottom and middle positions (T9, T7, T10, T12, T15, and T14). In the top range of the Z axis (T2, T4, and T5), the Y axis movement has more influence on the stiffness in the Y axis direction, which can also be a result of the interaction between Y and Z movement. These observations for the stiffness in the Y direction can be seen in Figure 8 as well as in the results presented in Figure 6 for this direction.

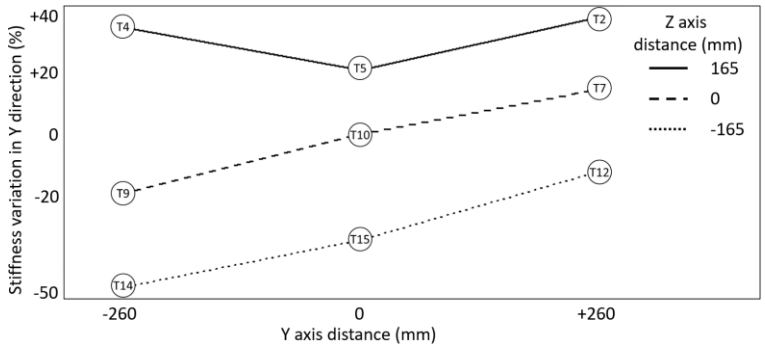

Figure 8. Influence of the interaction between the positioning of Y and Z axes in the stiffness in the Y direction.

In summary, the stiffness level for both X and Y direction is higher when the Z and Y axes are positioned at their higher values (i.e. T2). The highest and lowest stiffness value for both X and Y directions is presented in points T2 and

T14, respectively. This can be explained by the variation of the torsion/bending moment distance. The lower the Y and Z axes are positioned, the higher is the distance of the torsion/bending moment (i.e. T14).

These results show that the stiffness in the X direction is lower than in the Y direction, for any points with X axis positioned in the center of the table (i.e. X=0). At this condition, two torsion moments are applied in the X direction, while in the Y direction only one bending moment is applied. This results in higher deflections in the X direction than in the Y direction for the same load value. An example of this condition is presented in Figure 9.

In Figure 9a, a frontal view of the TCP without any applied load is presented and in Figure 9b, the same perspective is presented when a load is applied in both directions, X and Y. The displacement observed in the frontal view occurs in the X direction and is presented with amplification of 3500 times. In Figure 9c the TCP without any load applied is also shown, while in Figure 9d the respective displacement in the Y direction is presented. The amplification is kept as 3500 times, however, for X direction (Figure 9b) the displacement is higher (i.e. 237%) than in the Y direction (Figure 9d).

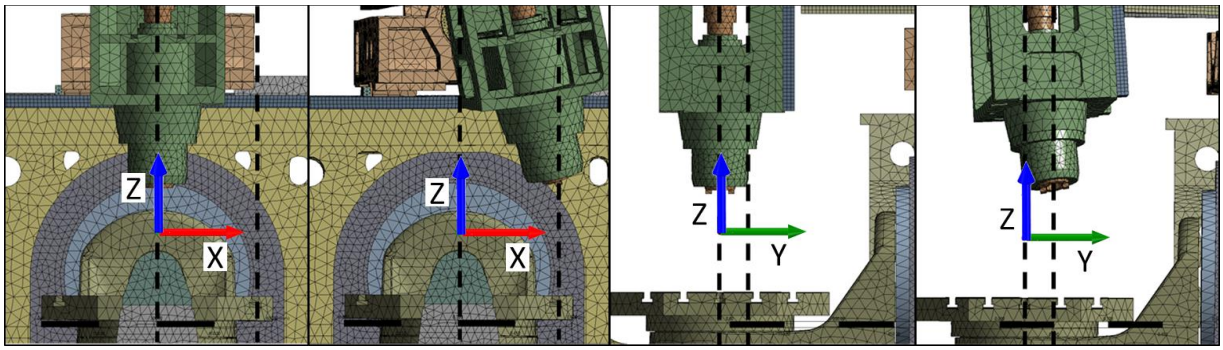

a) b) c) d)

Figure 9. Displacement at the reference point (T10) for application of 1 kN load in both X and Y directions: a) Frontal view of the TCP without load application; b) Displacement in the X direction; c) Right view of the TCP without load application; d) Displacement in the Y direction.

Referring to Figure 4b, the points that correspond to the locations where the Y axis position kept at the center of the table (i.e. Y=0) are T1, T3, T5, T6, T8, T10, T11, T13, and T15. The respective names and positions in the machine's work volume for all these tests are presented in Figure 10a. For these points, two different conditions can be observed: (1) when Y and X are equal to zero, and; (2) only the Y is equal to zero. The first case occurs in points T5, T10, and T15. In these cases, the stiffness behavior was already analyzed. For the other points (T1, T3, T6, T8, T11, and T13), there is an additional moment in the Z axis that will directly affect the stiffness level in the Y direction.

This additional moment exists because of the movement of the TCP in the X direction and the distance, which was zero in the points T2, T4, T5, T7, T9, T10, T12, T14, and T15, now has a different value. With this additional moment, the loads in the Y direction lead to two moments. The bending moment mentioned before still is present, but now a torsion moment in the Z axis also exists. This torsion moment decreases as the TCP is closer to the center of the table and increases as it gets farther from the center. Figure 10b shows the additional torsion moment caused by the X axis movement and the maximum and minimum stiffness for the Y=0 condition, T5 and T11, respectively.

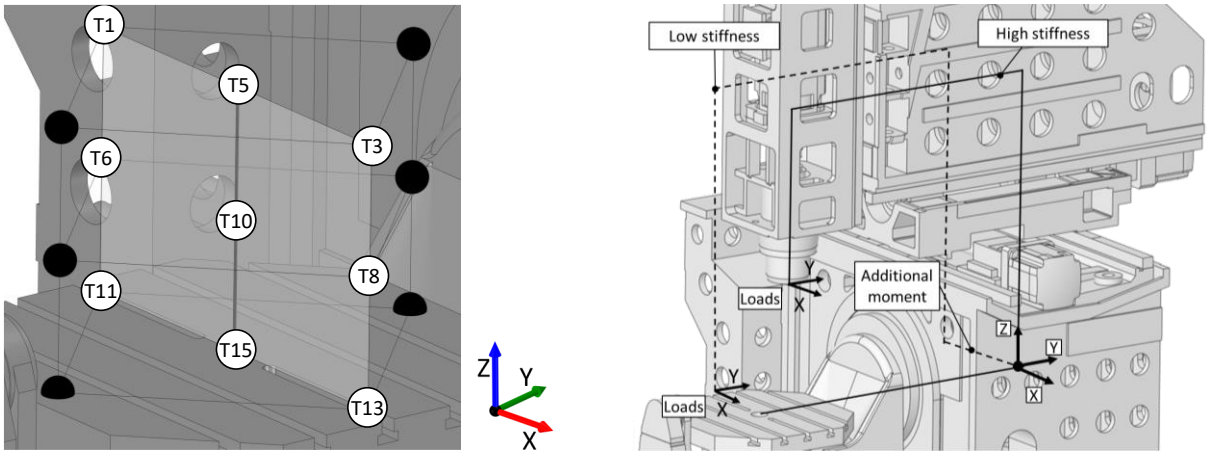

a) b)

Figure 10. a) Name and position of the tests with Y axis positioned in the center of the table; b) Points T5 and T11, an example of two different load conditions according to the X and Z axes movement.

A frontal view of the machine tool with the absolute values of the stiffness and its respective variation is presented in Figure 11. From the results, it is observed that the X and Z axes movement independently has a similar influence on the stiffness in the X axis direction. For constant positions of the Z axis, the stiffness in the X direction decreases around 30% from the top level of the Z axis (T1, T3, and T5) to the middle level of the Z axis (T6, T8, and T10), or from the middle level to the bottom level (T11, T13, and T15). For constant positions of the X axis, it decreases about 36% for each X position level; higher (T3, T8, and T13), middle (T5, T10, and T15), and lower (T1, T6, and T11). However, combining the Z and X axes movements the change in the stiffness level is more significant, around -55% from point T5 to point T13. These observations can also be seen in Figure 12 as well as in the results presented in Figure 11.

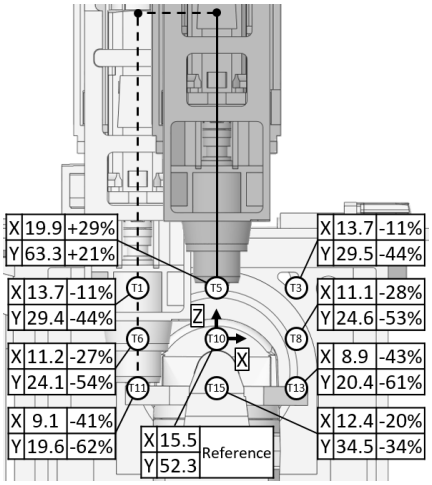

Figure 11. Stiffness absolute value in terms of N/μm and its variation in % for all points where the Y axis is positioned in the center of the machine's work volume.

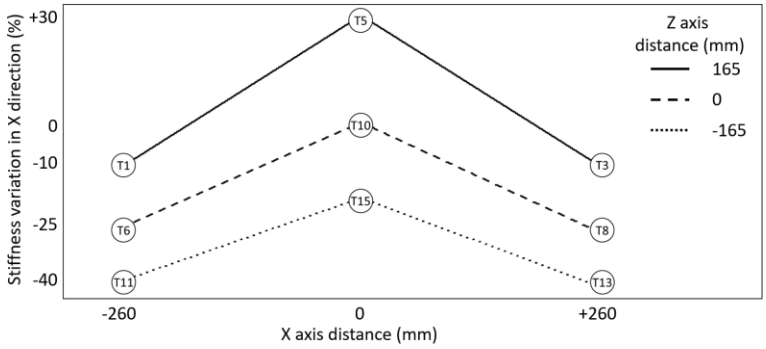

Figure 12. Influence of the interaction between the positioning of X and Z axes in the stiffness level in the X direction.

The variation of the stiffness in the Y and X direction has similar behavior, thus all these observations apply for the stiffness in both directions. However, for the stiffness in the Y axis direction, the X position has a larger influence, which is caused by the additional moment that originated when the X axis movement. In the points where this additional moment occurs (T1, T3, T6, T8, T11, and T3) the stiffness level is lower. The mentioned observations for the Y direction are observed in Figure 13 as well as in the results presented in Figure 11 for this direction.

The highest stiffness value for both directions (X and Y) is presented in point T5, which is explained by the load's moment; at this point, the loads applied in the Y direction do not cause a torsion moment. Moreover, at this point, the loads applied in the X direction have the lowest distance for both torsion moments, (i.e. in Z and Y axes). The lowest stiffness value for both directions (X and Y) occurs in the extreme points of the axis' position (T11 and T13). That is also explained by the load's moment, since in these cases the loads in X and Y directions have the highest moment distance. The loads in the Y direction have the additional moment in the Z axis, which also contributes to reducing the stiffness in this direction.

In summary, the stiffness in the X direction is lower than in the Y direction for any point. This is explained by the fact that for all points, the loads in X direction always cause two torsion moments. For loads in the Y direction, the conditions where torsion moment exists, lower stiffness values are presented. This indicates that the torsion moment has a higher influence than the bending moment, which also explains why X direction has lower stiffness for any situation.

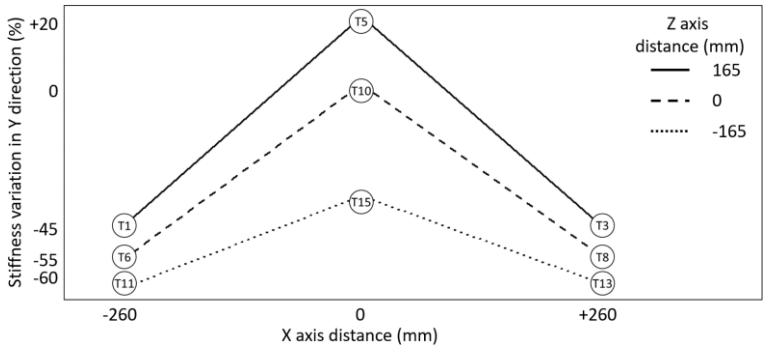

Figure 13. Influence of the interaction between the positioning of X and Z axes in the stiffness level in the Y direction.

The difference of the displacement in the Y direction with and without the torsion moment is shown in Figure 14. In Figure 14a, a right view of the point T5 without any applied load is presented, and Figure 14b shows the same point with 1 kN applied in both X and Y direction. These conditions, presented in Figure 14a and Figure 14b, do not have the additional torsion moment. Figure 14c and d present the conditions of point T11 that have the additional torsion moment. The unloaded condition is shown in a right view in Figure 14c, and the same perspective of the loaded condition is presented in Figure 14d. Both loaded conditions, Figure 14b and d are presented with amplification of 3500 times. However, the condition where the torsion moment exists (T11) results in a displacement 223% higher.

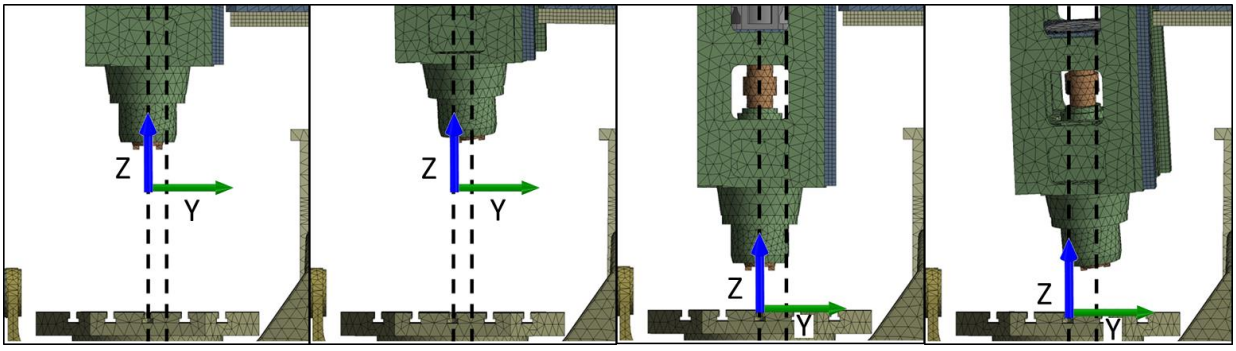

a) b) c) d)

Figure 14. Right view of the displacement in the Y direction for points T5 and T11: a) Point T5 without applied load; b) Displacement of T5 in Y direction for a load of 1 kN; c) Point T11 without applied load; d) Displacement of T11 in Y direction for a load of 1 kN.

4. CONCLUSIONS

Due to its mechanical structure, the machine's structural stiffness is highly affected by the axes' movement, thus different stiffness values result from different axes positioning in the machine's work volume. The machine's architecture also has a high impact on the stiffness in the X direction, which has lower values when compared to the Y direction. However, the stiffness in the Y direction has higher variation when compared to the X direction. This is a result of the additional moment existent when the X axis moves from the central point. Even with this high variation, the lower stiffness level in the Y direction is higher than in the X direction.

The highest stiffness level of the machine tool is presented when the X axis is positioned at zero, the Y and Z axes are positioned in their positive limits. The lowest stiffness level is presented when the Y axis is positioned at zero, the X axis is positioned in its positive or negative limit and the Z axis is in its negative limit. The stiffness level is highly influenced by the movements of the X axis when compared to the movement of the Y axis. However, the stiffness variation is equal if the X axis moves along its negative or positive direction, which does not happen in the case of the Y axis. The stiffness is reduced when the Y axis is moving along its negative direction and increases when moving along the positive direction.

Aligned to the current trends in global manufacturing system, the understanding of the stiffness behavior contributes to increase the reliability of the cutting process. Different strategies for the tool path or for the positioning of the part at the machine table can be proposed to increase the final process accuracy. Machined parts which can be affected by the high stiffness variation can be positioned at the machine table to avoid that. The process parameters can be adapted based on which region of the table the machine is positioned to increase the productivity. When applied in the design phases of the machine tool, the method allows to modify the machine's architecture to reduce the influence of axes' movement in

the machine's stiffness. This knowledge can also be applied as additional information for error compensation system, to compensate the error caused by the stiffness level.

5. ACKNOWLEDGEMENTS

To the Coordenação de Aperfeiçoamento de Pessoal de Nível Superior (CAPES) for the financial support of this research. To the Competence Center of Manufacturing and the Brazilian Aeronautics Institute of Technology for all the infrastructure provided for this research. The authors are also especially thankful to the machine tools manufacturer ROMI for all the technical discussion and all the equipment provided for this research.

6. REFERENCES

Abele, E., J. C. Aurich, B Behrens, D. Biermann, C. Brecher, U. Heisel, D. Heinisch, et al. 2013. "Measurement and Test Techniques." In *Process Machine Interactions: Predicition and Manipulation of Interactions between Manufacturing Processes and Machine Tool Structures*, edited by Berend Denkena and Ferdinand Hollmann, Berlin, 3–27. Berlin, Heidelberg: Springer. https://doi.org/10.1007/978-3-642-32448-2_1.

Archenti, Andreas. 2014. "Prediction of Machined Part Accuracy from Machining System Capability." *CIRP Annals - Manufacturing Technology* 63 (1): 505–8. https://doi.org/10.1016/j.cirp.2014.03.040.

Brecher, Christian, and Stephan Tobias Witt. 2004. "Static, Dynamic and Thermal Behavior of Machine Tools with Regard to HPC." In *High Performance Cutting: CIRP International Conference*, 227–42. Aachen: RWTH. https://doi.org/wzl00000136x.

Deng, Congying, Yun Liu, Jie Zhao, Bo Wei, and Guofu Yin. 2017. "Analysis of the Machine Tool Dynamic Characteristics in Manufacturing Space Based on the Generalized Dynamic Response Model." *The International Journal of Advanced Manufacturing Technology* 92 (1–4): 1411–24. https://doi.org/10.1007/s00170-017-0201-9.

Gao, Xianming, Baotong Li, Jun Hong, and Junkang Guo. 2016. "Stiffness Modeling of Machine Tools Based on Machining Space Analysis." *International Journal of Advanced Manufacturing Technology* 86 (5–8): 2093–2106. https://doi.org/10.1007/s00170-015-8336-z.

Huo, Dehong, Kai Cheng, and Frank Wardle. 2009. "Design of Precision Machines." In *Machining Dynamics: Fundamentals, Applications and Practices*, edited by Kai Cheng, London, 283–321. Springer. https://doi.org/10.1007/978-1-84628-368-0_10.

International Organization for Standardization. 2012. "ISO 230-1:2012: Test Code for Machine Tools - Part 1: Geometric Accuracy of Machines Operating under No-Load or Quasi-Static Conditions."

Koenigsberger, F. 1970. "General Specification of the Problems." In *MACHINE TOOL STRUCTURES*, edited by F. Koenigsberger and J. TLUSTY, 1st ed., 3–25. Hungary: Pergamon Press. https://doi.org/10.1016/B978-0-08-013405-5.50004-2.

Slocum, Alexander H. 1992. *Precision Machine Design*. Society of Manufacturing Engineers.

Soons, Johannes Augustinus. 1993. "Accuracy Analysis of Multi-Axis Machines." Technische Universiteit Eindhoven. https://doi.org/10.6100/IR400139.

Szipka, Károly, Theodoros Laspas, and Andreas Archenti. 2018. "Measurement and Analysis of Machine Tool Errors under Quasi-Static and Loaded Conditions." *Precision Engineering* 51 (January): 59–67. https://doi.org/10.1016/j.precisioneng.2017.07.011.

Weck, Manfred. 1984. Handbook of Machine Tools: Construction and Mathematical Analysis. Vol 2. Aachen: Wiley.

Zulaika, Juanjo, and Francisco Javier Campa. 2009. "New Concepts for Structural Components." In *Machine Tools for High Performance Machining*, edited by L. Norberto López De Lacalle and Aitzol Lamikiz, 47–73. London: Springer. https://doi.org/10.1007/978-1-84800-380-4_2.

7. RESPONSIBILITY NOTICE

The authors Tédni de Abreu Goulart, Jefferson de Oliveira Gomes e Ronnie Rodrigo Rego are the ones responsible for the printed material included in this paper.